Clumpy coexistence in phytoplankton: The role of functional similarity in community assembly

Caio Graco-Roza [1, 4]*, Angel M Segura [2], Carla Kruk [3], Patrícia Domingos [1], Janne Soininen [4], Marcelo Manzi Marinho[1]

[1] Laboratory of Phytoplankton of Ecology and Physiology, Department of Plant Biology, University of Rio de Janeiro State, Rua São Francisco Xavier 524—PHLC Sala 511a, 20550-900, Rio de Janeiro, Brazil. Telephone: +552123340822

[2] Modelización Estadística de Datos e Inteligencia Artificial (MEDIA) CURE-Rocha, Universidad de la República, Uruguay.

[3] Sección Limnología, IECA, Facultad de Ciencias, Universidad de la República, Uruguay.

[4] University of Helsinki, Department of Geosciences and Geography, PO Box 64, FI00014, Helsinki, Finland. *correspondence author: caiogracor@gmail.com

Abstract

Emergent neutrality (EN) suggests that species must be sufficiently similar or sufficiently different in their niches to avoid interspecific competition. Such a scenario results in a multimodal distribution of species abundance along the niche axis (*e.g.*, body size), namely clumps. From this perspective, species within clumps should behave in a quasi-neutral state, and their abundance will show stochastic fluctuations. Plankton is an excellent model system for developing and testing ecological theories, especially those related to size structure and species coexistence. We tested EN predictions using the phytoplankton community along the course of a tropical river considering (i) body size structure, (ii) functional clustering of species in terms of morphology-based functional groups (MBFG), and (iii) the functional similarity among species with respect to their functional traits. Considering body size as the main niche axis, two main clumps (clump I and II) were detected in different stretches of the river and remained conspicuous through time. The clump I comprised medium-sized species mainly from the MBFG IV, while the clump II included large-bodied species from the groups V and VI. Pairwise differences in species biovolume correlated with species functional redundancy when the whole species pool was considered, but not among species within the same clump. Within-clump functional distinctiveness was positively correlated with species biovolume considering both seasons, and also at the upper course. These results suggest that species within clumps behave in a quasi-neutral state, but even minor shifts in trait composition may affect their biovolume. In sum, our findings point that EN belongs to the plausible mechanisms explaining community assembly in river ecosystems.

Keywords: species coexistence; emergent neutrality; functional distinctiveness; functional redundancy

Introduction

Understanding the mechanisms promoting species coexistence and shaping community structure has been a long-standing goal in community ecology. The former idea that the number of coexisting species is limited by the number of growth-limiting resources or niche dimensions (Gause 1936, Hardin 1960), and its derivate idea, "*the paradox of the plankton*" (Hutchinson 1957), have been widely explained in terms of endogenous and exogenous spatio-temporal mechanisms (Roy and Chattopadhyay 2007). Trait-based approaches are useful to test this matter due to their potential to generalize patterns beyond species' identity, especially because traits influence the species' ability to acquire resources and persist through environmental changes (McGill et al. 2006, Díaz et al. 2013, 2016). Nonetheless, niche-based theory proposes that the environment filters community composition through species' ecological requirements, which can be perceived through species' traits. However, at small spatial scales, species interactions present a predominant role, as the environmental heterogeneity is expected to be small (Götzenberger et al. 2012). In contrast, the more recent neutral theory suggests that diversity results from random dispersal, speciation, and extinction rates with no role of niche differences in species coexistence (Hubbell 2001). This type of dynamics should then result in random distribution of functional traits along environmental gradients (Kraft et al. 2008, Cornwell and Ackerly 2009).

More recently, it was shown that community organization is driven by eco-evolutionary processes such as speciation and nutrient uptake kinetics resulting in groups comprising different species with similar ecological requirements(Gravel et al. 2006, Hubbell 2006, Scheffer and van Nes 2006). This finding led to the 'emergent neutrality hypothesis' (EN) (Holt 2006) that has been supported by observational studies, e.g., for phytoplankton from brackish waters (Segura et al. 2011), birds from the North of Mexico (Thibault et al. 2011),

and beetles at the global scale (Scheffer et al. 2015). EN suggests that species must be sufficiently similar, and thus, behave neutrally, or different enough in their niches to avoid competition. Such a scenario would result in species-rich aggregations or clumps along the niche axis (Scheffer and van Nes 2006, Vergnon et al. 2009, Fort et al. 2010). Modelling studies have shown that such predictions apply for both steady environmental conditions (Fort et al. 2010), and also fluctuating resource conditions (Sakavara et al. 2018). Empirical evidence about EN is still scarce, however (Scheffer et al. 2018).

The clumpy pattern arises from the species niche preferences, meaning that species within clumps occupy same niche and their abundances are distributed stochastically (Scheffer et al. 2018). However, within a clump, trait differences may be important to species performance in the niche space (McGill et al. 2006, Violle et al. 2007), and it is difficult to state whether species behave neutrally within clumps (i.e., when the strength of interspecific interactions equals the intraspecific interactions). Zooming in on the uniqueness of trait combinations of species, i.e. functional distinctiveness, within clumps may advance our comprehension of biotic interactions and move towards a measurable value of similarity at which species coexistence is driven stochastically. Functional distinctiveness reflects the non-shared functions among species within a given species pool (Violle et al. 2007), mirroring the concept of functional redundancy (Pavoine et al. 2017). However, although two functionally redundant species most likely show high similarity in trait combination, functional distinctiveness is not directly linked to redundancy (Coux et al. 2016, Ricotta et al. 2016, Violle et al. 2017). For example, two species could show similar functional distinctiveness, i.e. the degree at which a species differs from all the others within the species pool concerning their functional traits, and still not be similar in their trait composition at a pairwise level (Coux et al. 2016). This suggests that both functional redundancy and distinctiveness are good metrics to assess the role of trait combination in community

assembly. To this end, planktonic communities offer an excellenta highly interesting model for biodiversity theory testing due to their highly speciose communities and their known relationship between morphological traits and function (Litchman and Klausmeier 2008, Kruk and Segura 2012, Litchman et al. 2012).

Body size is considered as a master ecological trait and it is highly useful to characterize species niche (Downing et al. 2014). In phytoplankton, the body size is related to physiology and life-history (Litchman and Klausmeier 2008), photosynthetic processes (Marañón 2008), nutrient uptake kinetics (Litchman et al. 2010)and other eco-evolutionary processes (Sauterey et al. 2017). Despite the importance of body size, the use of a single trait as a proxy for the niche may not evidence species differences generated by hidden niches and impair the understanding of clumpy patterns (D'Andrea et al. 2018). The use of multiple traits emerges as a powerful tool to disentangle plankton functional structure and evaluate competing hypotheses (Reynolds et al. 2014, Chen et al. 2015, Bortolini and Bueno 2017). Morphology-based functional groups (MBFG) classification of phytoplankton species (Kruk et al. 2010) uses a is a multidimensional combination of morphological traits that cluster organisms into seven groups with similar physiology and ecological responses (Kruk et al. 2011), potentially overcoming the limitations of using a single trait dimension only. Assessing the uniqueness in trait combinations of species within the same functional cluster (e.g., clumps, MBFGs) could help to study the existence of functional equivalence (i.e., neutrality) among species. Overall, the functional distance among species is a useful tool to compare species in a multidimensional space by comparing species' functional differences, particularly because the environment may filter different functional traits across space and time (Mouillot et al. 2013, D'Andrea et al. 2020).

Riverine ecosystems are highly heterogeneous andsystems characterized by a continuous water flow that affects the morphology, sedimentation patterns, dispersal, and phytoplankton diversity (Reynolds and Descy 1996, Wetzel 2001). Several theories explain the longitudinal occurrence and abundance of river phytoplankton communities, such as River Continuum (Vannote et al. 1980) and Flood Pulse (Junk et al. 1989) concepts. However, an explicit study of community size structure and phytoplankton species coexistence under EN in riverine ecosystems is lacking. For example, phytoplankton species should attain higher biomass at the middle reaches or in the upper reaches of low-gradient stretches, and the continuous water flow reduces the likelihood of biotic interactions (Reynolds et al. 1994). However, the physiological and morphological characteristics of species within the local species pool may result from eco-evolutionary processes that cluster species into limited functional groups that are favored under specific environmental conditions (Scheffer et al. 2015). Here, we push forward three hypotheses to be tested in a tropical river by investigating phytoplankton community size structure both seasonally and spatially:

H_1 – There are peak aggregations of species abundance (i.e., clumps) along the body size axis of phytoplankton in the river that remain constant across space and time as a result of eco-evolutionary processes.

H_2 – Differences in species biovolume scales positively with functional redundancy at the community-level but not at the clump level, because species within the same clump behave in a quasi-neutral state. Hence, the dominance within clump varies stochastically between redundant species because fitness differences would be negligible within clumps.

H_3 – There is a positive relationship between species abundance and species functional distinctiveness within clumps. Though abundance fluctuates stochastically at pairwise level, the number of species holding similar trait combinations may affect the likelihood of the

interactions within clumps. Therefore, species with the most distinct trait combinations with respect to their clump peers are less likely to share same ecological requirements, and by consequence, attain higher abundance.

Methods

Study area

Samples were taken monthly at nine stations along the Piabanha river between May 2012 and April 2013. Piabanha river is in the tropical region of Brazil and has a drainage basin of approximately 4500 km² (Figure 1). The headwater is on Petrópolis at 1546m altitude and drains to the medium valley of Paraíba do Sul river crossing three cities and with agricultural activities in their watershed. We set three river stretches (lower, medium and upper courses) based on the location of steep slopes the river elevation profile (Figure 1). Data from two meteorological stations, located close to the sampling sites, were used to measure rainfall. We analyzed meteorological data up to three days before each sampling campaign. We classified seasons as dry season (May - October) and a wet season (November – April) based on the rainfall data.

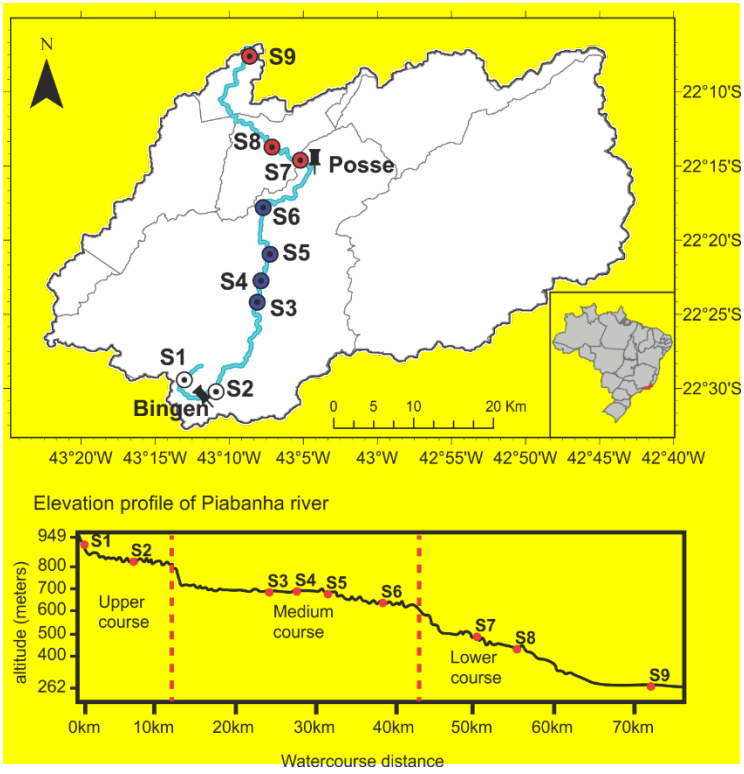

Figure 1. Map of the study area. The watershed area of the Piabanha river showing the river course (blue line) and the sampling sites colored according to river stretches (white circles = upper course, blue circles = medium course, red circles = lower course). The vertical dotted red line in the elevational profile figure indicates the locations of steep slopes used to define the boundaries of the river stretches.

Sampling and sample analysis

In the field, we measured temperature (°C), dissolved oxygen (DO, mg L^{-1}) and turbidity by a multiparameter probe sonde (YSI model 600 QS). Water discharge (WD, m^3 s^{-1}) was measured with the SonTek RiverSurveyor – M9. Furthermore, water samples were taken and kept frozen (one or 2 weeks) until the laboratory analysis for ammonium ($N{\cdot}NH_4^+$,mg L^{-1}), nitrate ($N{\cdot}NO_3^-$,mgL^{-1}), total phosphorus (TP, mg L^{-1}) and soluble reactive phosphorus (SRP, mg L^{-1}). The water samples were filtered (except for total phosphorus analysis) using borosilicate filters (Whatman GF/C), and nutrient concentrations were measured following

(APHA 2005). A complete description of the spatial and temporal patterns of the environmental variables measured in the Piabanha river can be found elsewhere (Graco-Roza et al. 2020).

Phytoplankton samples

Subsurface samples of phytoplankton were collected with a bottle of 200 mL and fixed with Lugol. In the laboratory, phytoplankton species were identified, and population densities estimated under an inverted microscope (Olympus CKX41) (Utermöhl 1958). At least 100 individuals of the dominant species were counted in each sample (error < 20%, $p < 0.05$, (Lund et al. 1958, Uhelingher 1964). Biovolumes ($mm^3\ L^{-1}$) were estimated by multiplying the density of each population by the average volume (V, μm^3), estimated from 20 random chosen individuals (whenever was possible), using the appropriate geometrical forms (Hillebrand et al. 1999, Sun and Liu 2003). In addition to the volume, we measured species' surface area (S, μm^2), the maximum linear dimension (MDL, µm), and the presence of aerotopes, mucilage, flagella, and siliceous exoskeleton. Hence, we used the volume and surface area of the species to estimate the individual surface volume ratio (SV). Species were then classified into Morphological Based Functional Groups (MBFG) according to (Kruk et al. 2010).

Traits-environment relationship

We tested the relationship between functional traits and the environmental variables using an RLQ analysis (Dolédec et al. 1996). The RLQ allows the visualization of the distribution of species traits and their related ecological preferences by testing the co-inertia between the matrices of environmental variables (R), species abundances (L), and species traits (Q). A Monte Carlo permutation test with 999 permutations at $\alpha = 0.05$ was used to test the statistical

192 significance of the RLQ axes. Furthermore, a fourth-corner method was applied to test the
193 statistical significance of all pairwise associations between species functional traits and
194 environmental variables. We quantified the strength of the associations using Pearson
195 correlation coefficient r_p, and the global statistics F-value (Legendre et al. 1997). The p-
196 values were corrected with 49999 permutations of the sites and the species to correct type I
197 errors, using false discovery rate method for adjusting p-values to control overall error rate
198 (Dray et al. 2014). However, because RLQ does not provide a significance test to identify
199 which combination of environmental variables acts on which combination of functional traits,
200 and the fourth-corner analysis tests the functional traits one at a time without considering the
201 covariation among traits and environmental variables, we used also a combined method of
202 RLQ and fourth-corner analysis (Dray et al. 2014). The significance of the associations was
203 tested by 99999 permutations of the sites and the species (Dray and Legendre 2008) to
204 correct type I errors, using false discovery rate method for adjusting p values to control the
205 overall error rate (Dray et al. 2014).

206 *Clumpy patterns*

207 To test for the existence of peak aggregations of species abundance along the body size axis
208 of phytoplankton - $\mathbf{H_1}$, we analyzed the community structure in each season (dry and wet) and
209 river stretches (upper, medium, and lower course). First, the individual volume of species was
210 log-transformed (log_2) and used as the main niche axis (X= log_2 volume). Hence, we divided
211 the niche axis into equally spaced segments (one segment per unit of log_2 biovolume) and for
212 each segment (j), we estimated the Shannon entropy (H) using the biovolume of the observed
213 species (Fort et al. 2010, Segura et al. 2011). The entropy index was defined as:

214 $$H_j = \sum_{i=1}^{n} p_i \, log_2(p_i), \quad (1)$$

215 where p_i is the fraction of biovolume of species *i* in the community of *n* species. Finally, we

tested the significance of the entropy (*H*) by comparing the observed *H* against an expected uniform distribution under the null hypothesis of homogeneous *H*. For this, we created 1000 communities by sampling the volume of species from a random uniform distribution bounded by observed individual volumes. Then, each species had a biovolume assigned to it, which was taken from a randomization of the observed biovolume matrix, keeping both the empirical species rank-abundance pattern and total biovolume in the sample. For each segment, the observed *H* was compared with the distributions of *H* generated under the null hypothesis, with significance defined according to standard 5% criterion (Fort et al. 2010; Segura et al. 2011).

Functional redundancy

To test whether differences in species biovolume scales positively with functional redundancy – **H_2**, we first calculated the functional redundancy (F_{Red}) and the differences in biovolume between pairs of species using the whole community and using only the species from the clumps with significant entropy values. The functional redundancy was obtained by calculating Gower's general similarity coefficient [function *gowdis*, R package FD (Laliberté et al. 2014)] on the species functional traits. We used Gower's dissimilarity (*Gd*) because it can handle mixed variable types (continuous, binary, ordinal and categorical traits). *Gd* defines a distance value d_{jk} between two species as

$$d_{jk} = \frac{1}{N}\sum_{i=1}^{n}\left|\frac{(x_{ij}-x_{ik})}{max(x_i)-min(x_i)}\right|, \quad (2)$$

where, N is the number of functional traits considered, x_{ij} the value of trait i for species j and x_{ik} the value of the trait i for species k. We thus tested **H_2** by conducting Mantel tests [function *mantel*, R package vegan (Oksanen 2017)] with 1000 randomizations, whenever

possible, on F_{Red} and $Diff_{Biov}$ matrices using all species, and separately for the species of each significant clump.

Functional distinctiveness (F_{Dist})

To test whether there is a positive relationship between species relative abundance at clump-level and species functional distinctiveness – **H_3**, we estimated the functional distinctiveness (F_{Dist}) as the distance of a species to the average trait position (centroid) in the multidimensional functional space for the set of species pertaining to each of the significant clumps using the equations proposed by Anderson (2006). First, we obtained species coordinates in the functional space by applying a Principal Coordinates Analysis (PCoA) in the species-by-traits data table using the Gower's dissimilarity (*Gd*). Hence, the distance from a species to its given centroid was calculated as

$$z_{ij}^{c} = \sqrt{\Delta^2\left(u_{ij}^{+}, c_{i'j'}^{+}\right) - \Delta^2\left(u_{ij}^{-}, c_{i'j'}^{-}\right)}, \quad (3)$$

where Δ^2 is the squared Euclidean distance between u_{ij}, the principal coordinate for the *j*th point in the *i*th group, and c_i, the coordinate of the centroid for the *i*th group. The super-scripted '+' and '-' indicate the real and imaginary parts respectively (Equation 3, see Anderson 2006 for details). We did not weight the clump-centroid by species abundance and calculated F_{Dis} using all species pertaining to the significant clumps. Hence, to test **H_3**, we modeled the relationship between species biovolume and F_{Dist} using linear models. We used biovolume as response variable, with F_{Dist}, Clump position, and seasonal or spatial categories as fixed factors. Because the aggregation of sites across space and time have a nested design (i.e. spatial aggregation comprises all months sampled, and temporal aggregations comprises all sites sampled), we modelled spatial and temporal categories separately.

Results

Our samples included 150 species that were classified in six (MBFG I, III, IV, V, VI, and VII) from the seven MBFGs based on their functional traits (Table 1). Species traits were significantly associated with environmental variables (RLQ analysis; Figure 3; $P < 0.05$). Individual volume (V), surface volume ratio (SV), maximum linear dimension (MLD), and siliceous exoskeleton (Si) correlated significantly with the first axis, where SV had the highest correlation ($r = -0.10$). Also, MLD and flagella correlated significantly with the second axis ($r = -0.07$, $r = -0.08$). For the environmental variables, water temperature (T) and water discharge (WD) correlated the strongest with the first axis ($r = 0.10$ for both variables), which also correlated significantly ($p < 0.05$) with total phosphorus (TP), dissolved oxygen (DO), turbidity (Turb), and pH. In addition, dissolved inorganic nitrogen (DIN), soluble reactive phosphorus (SRP), and turbidity (Turb) correlated significantly with the second axis, and Turb had the highest correlation ($r = 0.90$) (Figure 2A).

Table 1. Distribution of species among the morphological-based functional groups.

MBFG	Number of species	Representative taxa
I	9	*Chroococcales* sp, *Chroococcus* sp.
III	3	*Limnothrix* sp.
IV	60	*Pseudoanabaena limnetica*, *Pseudoanabaena catenata*
V	13	*Euglena* sp. *Cryptomonas* sp.
VI	57	*Cymbella* sp., *Synedra* sp.
VII	8	*Dictyosphaerium* sp.
Total	150	

The distribution of the species belonging to different MBFGs in the RLQ ordination (Figure 2B) reflect their occurrence in relation to the environmental variables. The groups IV, V and VI included 87% of the total number of species. Species from the group IV included filamentous, colonial and unicellular species ranging from 21 μm^3 to 8181 μm^3 with no specialized morphological traits (e.g. flagella, Si). Group V comprised unicellular flagellated

species ranging in size from 31µm³ to 31864 µm³, and group VI included unicellular and chain-forming species with siliceous exoskeletal body that ranged from 48µm³ to 19045µm³. According to the fourth-corner analysis, MLD was negatively correlated with pH (r = -0.09) and WD (r = -0.10), flagella was negatively correlated with Turb (r = -0.08), Si was positively correlated with Turb (r = 0.11) and WT (r = 0.09), whereas V was positively correlated with Turb (r = 0.08) (Figure 2C).

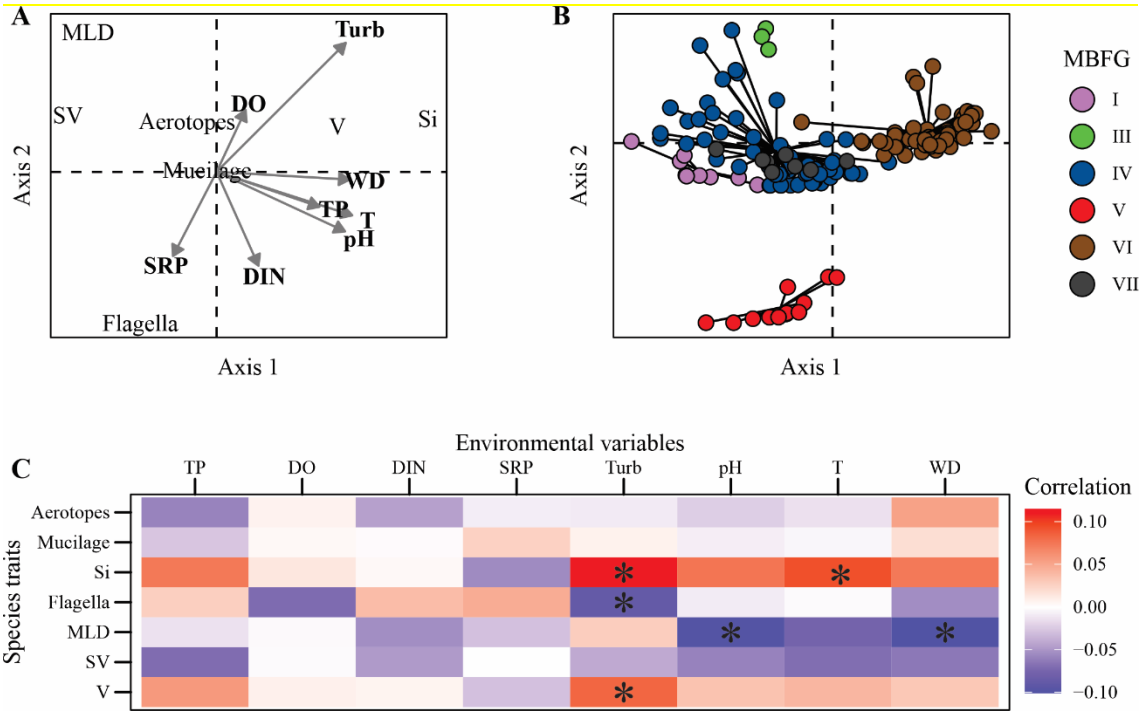

Figure 2. Results of the RLQ and fourth-corner analysis. (A) The relationships between species traits and environmental variables. First and second axes summarized 64.9% and 20.7% of variation, respectively. (B) The distribution of species in the functional space. Each point in the ordination plot within clusters represents the position of a species modelled according to its traits on RLQ axes 1 and 2. (C) The bivariate relationships between species traits and environmental variables. Functional traits are abbreviated as: Si = siliceous exoskeleton, MLD = maximum linear dimension, SV = surface volume ratio, V = individual volume. Environmental variables are abbreviated as: TP = total phosphorus, DO = dissolved

oxygen, DIN = dissolved inorganic nitrogen, SRP = soluble reactive phosphorus, Turb = turbidity, T = water temperature, WD = water Discharge.

The groups IV, V, and VI contributed to 95% of the mean biovolume of total phytoplankton in dry and wet seasons, and 96.6% across river stretches (Figure 3). The group VI had the highest contribution for the biovolume of almost all river stretches in both seasons, except for the upper course during dry season was dominated by the group IV (Figure 3). The entire list of species, functional traits, and assigned MBFG can be found in Table S1.

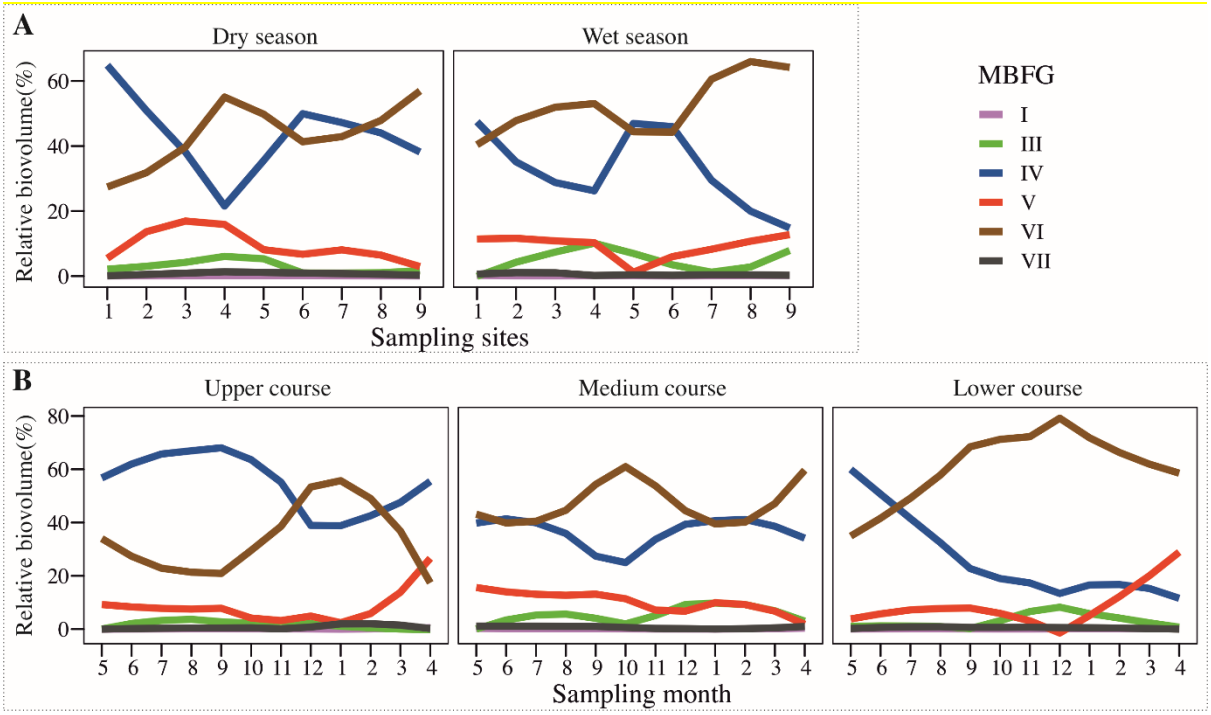

Figure 3. Relative contribution of morphology-based functional groups (MBFG) to total biovolume observed along the seasons and river stretches of the Piabanha river between May-2012 and April-2013. Trend lines are loess curves fit of each MBFG.

Overall, species individual volume ranged from 4.19 µm³ to 31864 µm³ totaling 14 equally spaced segments (S) of volume along the niche axis. From the 14 segments, three of them

showed significant entropy values, specifically S9, S13, and S14. This resulted in a biovolume aggregation (i.e. clumps) in two regions of the niche axis considering both temporal (Figure 4) or spatial categories (Figure 5). The first clump (Clump I) comprised species mainly from the group IV from S9 (e.g., *Pseudoanabaena limnetica*, *Pseudo anabaena catenata*), whereas the second clump (Clump II) included species from groups V and VI (e.g., *Euglena* sp., *Cymbella* sp.) at the segment S14. However, during the wet season, a few species from S13 also had significant entropy values and therefore were included in the clump II (Fig 4B).

The mean biovolume of species within clumps differed across seasons, but the identity of the most abundant species did not vary. *Pseudanabaena* sp. 4 (spp. 28) and *Pseudanabaena catenata* (spp. 12) had the highest biovolumes of clump I and held the highest biovolumes of the clump at both dry and wet seasons. Within the clump II, *Synedra* sp. (spp. 80) attained the highest biovolume during the dry season, whereas *Cymbella* sp. (spp. 051) contributed the most to clump biovolume in the wet season.

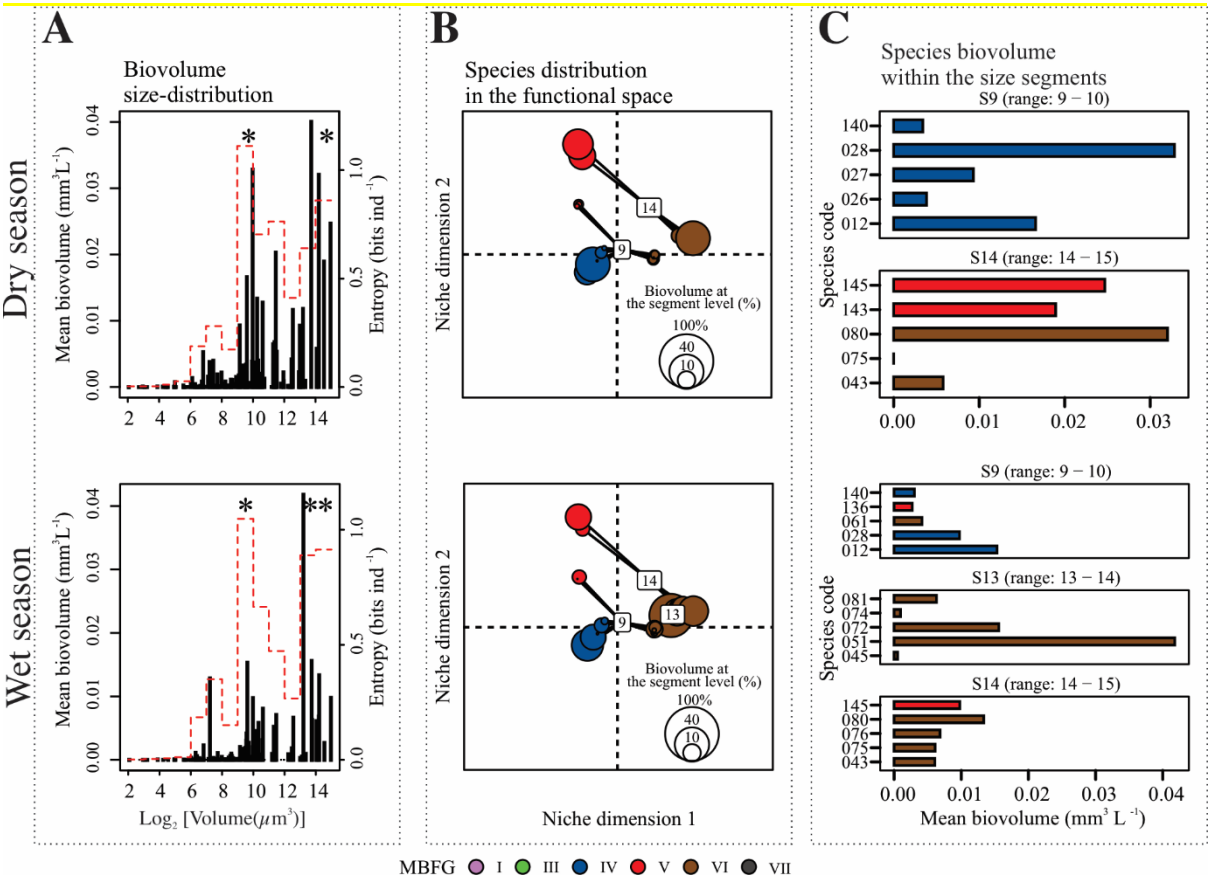

Figure 4. Distribution of phytoplankton biovolume along the body size axis, the ordination of species from the significant size segments (S) in the functional space, and the mean biovolume of the five most abundant species of each significant size segment during the dry and wet seasons of the Piabanha river, RJ. (A) Stem plots show size distribution in the sampling sites of the river Piabanha. Each stem represents a species with its body size (in $\log_2$) plotted on the abscissa and the mean biovolume plotted on the ordinate. The red dotted line indicates the entropy value of each size segment (i.e., one unit of $\log_2$ volume), and the asterisk highlights the significant entropy values tested through 1000 randomizations. (B) The species of the corresponding significant size-segment are ordinated in the functional space. The size of the circles represents the species contribution to the total biovolume of the size segment. (C) Bar plots (right show the biovolume of the five most abundant species from each significant size segment. Species are colored according to their morphology-based

functional groups (MBFG). The code of each species can be found in the supplementary material, Table S1.

Regarding the river stretches, *Pseudoanabaena* sp. 4 and *Pseudoanabaena catenata* contributed the most to the biovolume of the upper course, and only the clump I had significant entropy values for species from the S9 (Figure 5A). At the medium course, both the clump I and II had significant entropy values, mainly due to species from the S9 with *Pseudoanabaena* sp. 4 as the most abundant, and from the S14 with *Synedra* sp. as the most abundant (Figure 5B). At the lower course, the clump II had significant entropy values, specifically at the S14 where *Synedra* sp. contributed most to biovolume at segment level (Figure 5C).

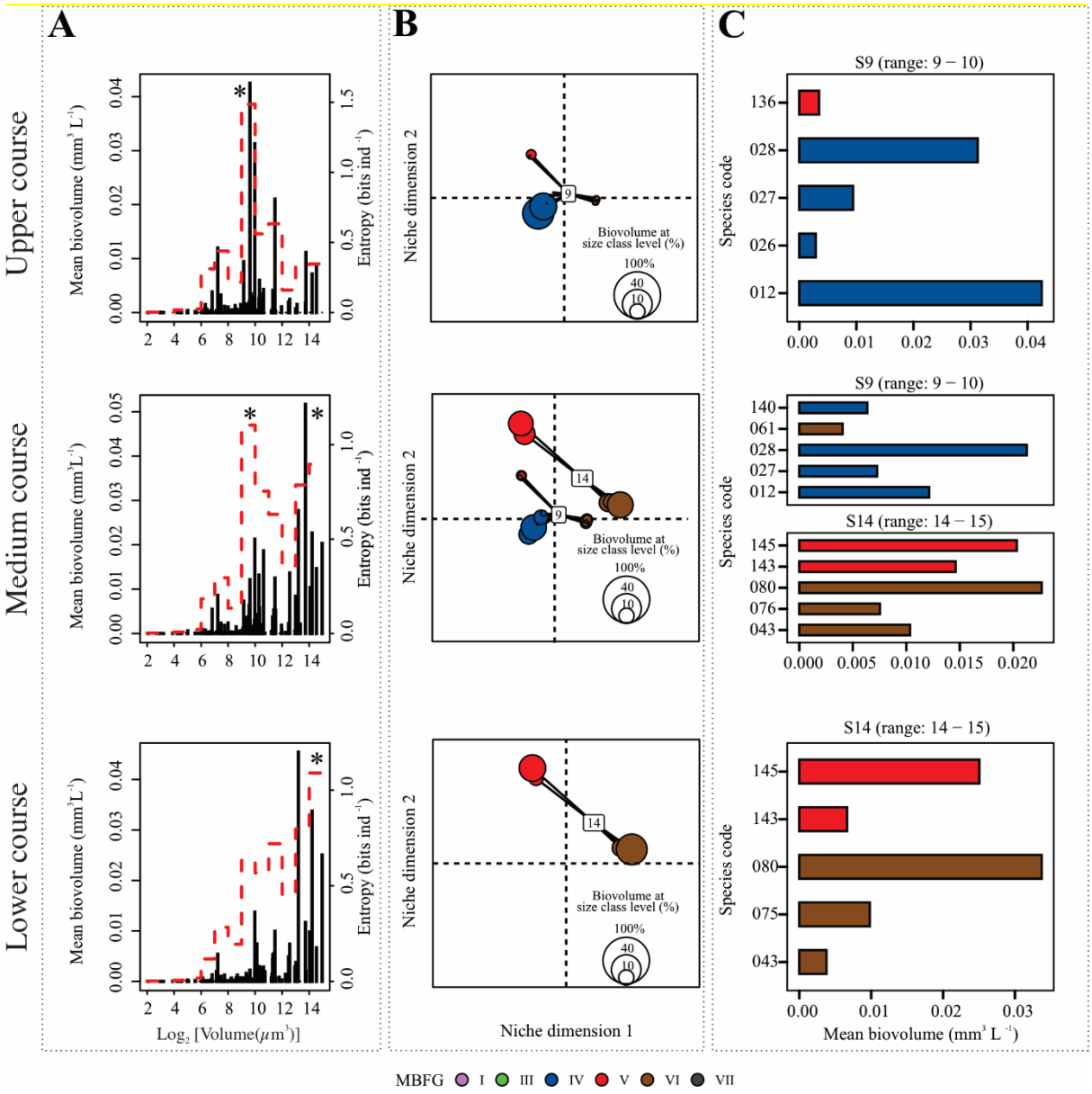

Figure 5. Distribution of phytoplankton biovolume along the body size axis, the ordination of species from the significant size segments (S) in the functional space, and the mean biovolume of the five most abundant species of each significant size segment at the upper, medium, and lower courses of the Piabanha river, RJ. (A) Stem plots show size distribution in the sampling sites of the river Piabanha. Each stem represents a species with its body size (in $\log_2$) plotted on the abscissa and the mean biovolume plotted on the ordinate. The red dotted line indicates the entropy value of each size segment (i.e., one unit of $\log_2$ volume), and the asterisk highlights the significant entropy values tested through 1000 randomizations.

348 (B) The species of the corresponding significant size-segment are ordinated in the functional
349 space. The size of the circles represents the species contribution to the total biovolume of the
350 size segment. (C) Bar plots (right show the biovolume of the five most abundant species from
351 each significant size segment. Species are colored according to their morphology-based
352 functional groups (MBFG). The code of each species can be found in the supplementary
353 material, Table S1.

354 Differences in biovolume among species were positively related to the functional redundancy
355 at the whole-community level, but not at the clump-level irrespectively to the season or river
356 stretch studied (Table 2). At the clump-level, we observed that species with higher
357 distinctiveness attained the highest biovolume in all the seasons and river stretches (except for
358 the lower course). The upscaling of biovolume with functional distinctiveness was observed
359 for species from both clumps, at different seasons and river stretches, but was particularly
360 different in the wet season, where species from clump II did not show any significant
361 relationship with biovolume, and at the medium and lower courses, where there were no
362 significant trends (Table 3).

363 **Table 2. Mantel correlation results.** Mantel correlation between the differences in species
364 biovolume and functional redundancy for the overall set of species and significant clumps
365 along the seasons (dry and wet) and river stretches (upper, medium and lower courses).

Seasons and river stretches	Stratum	Mantel correlation
Dry season		
	Overall	**0.180 (0.001)**
	Clump I	0.130 (0.120)
	Clump II	-0.172 (0.709)
Wet Season		
	Overall	**0.230 (0.001)**
	Clump I	0.065 (0.235)
	Clump II	-0.167 (0.705)
Upper course		

	Overall	**0.165 (0.002)**
	Clump I	0.065 (0.242)
Medium course		
	Overall	**0.171 (0.001)**
	Clump I	0.059 (0.217)
	Clump II	-0.168 (0.633)
Lower course		
	Overall	**0.258 (0.001)**
	Clump II	-0.167 (0.696)

Note: Significant ($p < 0.05$) values are in bold and p-values are inside parentheses

Table 3. Linear model results. Regression parameters of the relationship between species biovolume and functional distinctiveness at the clump level.

	Dependent variable: Log_{10} Biovolume				
	Biovolume				
	Dry season	Wet season	Upper course	Medium course	Lower course
F_{Dist}	14.925*	15.854*	24.440**	12.377	7.267
	(6.127)	(6.015)	(7.816)	(6.085)	(4.373)
Clump II	4.676	7.501*	9.619	4.373	2.067
	(6.148)	(3.175)	(18.074)	(5.169)	(3.689)
F_{Dist} × Clump II	-8.458	-15.863	-21.301	-7.911	-1.651
	(15.608)	(7.734)	(46.232)	(13.329)	(9.501)
Intercept	-8.979**	-9.748**	-12.951**	-7.945**	-6.165**
	(2.439)	(2.496)	(3.143)	(2.418)	(1.734)
Observations	26	31	19	28	26
R^2	0.420	0.437	0.457	0.374	0.579
Adjusted R^2	0.341	0.374	0.348	0.296	0.522
Residual Std. Error	0.756 (df = 22)	0.663 (df = 27)	0.823 (df = 15)	0.755 (df = 24)	0.523 (df = 22)
F Statistic	5.313**	6.987**	4.204*	4.778**	10.090**

	(df = 3; 22)	(df = 3; 27)	(df = 3;15)	(df = 3;24)	(df = 3; 22)
Note:					$^{*}p < 0.05$ $^{**}p < 0.01$

366 **Discussion**

367 Present results showed that (i) the clumps in body size are a conspicuous feature of
368 phytoplankton community structure in riverine systems across seasons and river stretches; (ii)
369 species within clumps show random distribution of biovolume with respect to their pairwise
370 functional differences, but functional redundancy is related to differences in biovolume at the
371 whole-community level; and (iii) species biovolume generally scales positively with
372 functional distinctiveness at the clump level. Note that, on the one hand, multimodal
373 aggregation of species biovolume along body size axis only points to the integration of niche-
374 based processes and neutrality driving community assembly (Vergnon et al. 2009), but it does
375 not imply that EN is the only mechanism behind phytoplankton coexistence. On the other
376 hand, our results do not support alternative hypothesisexplanations such as pure neutrality
377 (Hubbell 2001) or high dimensional hypothesis (Clark et al. 2007) because pure neutrality
378 predicts a uniform distribution of species biovolume along the niche axis (Hubbell 2001), and
379 the HDH does not predict any particular trait distribution (Vergnon et al. 2009, Ingram et al.
380 2018).

381 One alternative theory that is likely to explain clumpy aggregations is the Holling's textural
382 hypothesis (Holling 1992). The textural hypothesis explains multimodal species size
383 distribution with environmental constraints, and although distribution of the clumps was
384 spatially structured, our results do not support HDH as a whole. River stretches and seasons
385 are radically different in river hydrology, nutrients and fluxes, but that was not reflected in
386 phytoplankton size structure. Moreover, if landscape controls the body size pattern alone,
387 differences in phylogenetics, biogeography, energeticsenergenitics, and community

388 interactions should not significantly affect such pattern (Allen et al. 2005). However, the
389 clumps in our data were in the similar size range and comprised species from the same
390 MBFG found in previous studies from different systems (Segura et al. 2011, 2013). More
391 importantly, there was a clear functional differentiation of species between clumps in terms
392 of MBFG (Figure 5-6), and the trait composition of the communities reflected adaptations to
393 survive in different environmental templates (Kruk and Segura 2012). For example, species
394 from the group IV dominated in low-flow waters with high nutrient input, while species from
395 group V and VI show different adaptations to survive in turbulent and mixed conditions
396 (Margalef 1978, Soares et al. 2007, Bortolini and Bueno 2017). Therefore, our findings
397 corroborate our $\mathbf{H_1}$ on the existence of significant peak aggregations in species biovolume
398 along the body size axis. Such results agree with previous evidence of EN using
399 phytoplankton as the model community in coastal and estuarine environments (Segura et al.
400 2011, 2013), and shows that clumpy distributions are evident on the phytoplankton
401 communities of riverine ecosystems presenting fluctuations in environmental conditions. In
402 addition, our findings are in line with recent modeling results suggesting clumpy patterns
403 arise in environments subjected to resources fluctuation (Sakavara et al. 2018). It remains to
404 be tested the trade off between resources among competing species, which is the remaining
405 ingredient for the emergence of clumps.

406 We expanded the level of analysis from mere size structure towards the inclusion of new trait
407 dimensions by analyzing the functional similarity at MBFG classification level and functional
408 redundancy. We found that the species from the same clump represent a selection of all the
409 possibilities amongst MBGFs, reinforcing that body size is a good proxy for niche
410 preferences of the species (Blanckenhorn 2000). However, assessing MBFGs helped to
411 assign niche differences at a finer degree, taking into account that using only a single trait
412 could impair the patterns behind community assembly (D'Andrea et al. 2018). Species within

413 the same MBFG are expected to share ecological strategy (Kruk et al. 2010, Kruk and Segura
414 2012) and accordingly to EN, would also perform similarly (Scheffer et al. 2018). Still, the
415 importance of traits to equalize or stabilize niche differences are context-dependent and
416 assessing the functional multidimensional space should help to unveil community assembly
417 processes (Bonser 2006). Here, we found that size-related traits (volume, MLD) and the
418 presence of flagella or siliceous exoskeleton were the main drivers of phytoplankton
419 distribution. Not surprisingly, such traits are key determinants on the assignment of species to
420 the main MBFG observed here (Kruk et al. 2010). Furthermore, we found that fitness
421 differences were significant at the community level, but not at within-clumps level, even
422 considering multiple morphological traits. Still, the dominance of medium-sized species
423 (clump I) in the upper course and of large-bodied species (clump II) in the lower course
424 suggests that the coexistence of these MBFGs tends to generate clumpy distributions that are
425 eroded when the ecosystem properties favor the dominance of other MBFGs, but the
426 fluctuations in biovolume within clumps remains stochastic even when clumps hold a few
427 species belonging to different MBFGs. These findings corroborate our **H2** - differences in
428 species biovolume scales positively with functional redundancy at the community level but
429 not at within-clumps level - and reinforces the predictions on the quasi-neutrality state of
430 species within clumps (Holt 2006).

431 We also outlined the role of functional similarity in community assembly by studying the
432 effects functional distinctiveness on species biovolume at clump level. We found that at the
433 clump I, species biovolume increased with functional distinctiveness, but this pattern was
434 weaker within clump II. Despite the species from group V and VI show lower growth rates
435 than the species from group IV (Kruk et al. 2010), their elongated shape provides advantage
436 under turbulent conditions (Reynolds et al. 1994) favoring these species under high flow
437 conditions on nutrient-rich environments (Irwin et al. 2006). Furthermore, nutrients are

hardly limiting phytoplankton growth especially in meso- or eutrophic rivers (Reynolds 2006), and large-bodied species are mostly randomly introduced from different habitats (e.g. periphyton or epiphyton) (Wang et al. 2014, Descy et al. 2017), which brings some uncertainty to the assumption of niche overlap due to size similarity. In fact, nutrients were not relevant for structuring the phytoplankton community of the Piabanha river, and we also observed a significantly different size-segment (S13) within the clump II during the high flow periods. Thus, one cannot be sure if species within clump II are truly occupying same niche or if they just were introduced to the plankton by random displacement. We suggest this may be the mechanism leading to the weak relationship between functional distinctiveness and biovolume within clump II.

Emergent neutrality results from eco-evolutionary processes that leads species selection towards a limited number of functional groups (Scheffer and van Nes 2006). This implies that the clumps observed here are not likely a result of competitive exclusion at the Piabanha river, but a convergent evolution of competing species over time as previously suggested (Macarthur and Levins 1967). Therefore, even when the competition rates are relaxed due to sufficient nutrient supply, some other limiting factors that are not consumed by biotic organisms such as heat energy or turbulence determine species biovolume, and even minor shifts in species trait combination may lead to higher biovolume with respect to other species occupying same niche. Our results showed that it is also possible to predict the biovolume of species within clumps, but only when neutral processes (e.g., species displacement) are relaxed and biotic interactions are more likely to occur. Therefore, our findings partially agree with $\mathbf{H_3}$ - there is a positive relationship between species abundance and species functional distinctiveness within clumps, but the environmental conditions seem to play a key role in the outcome.

In summary, we provided evidence of both neutral and niche perspective driving planktonic community assembly and support the view that emergent neutrality is a likely mechanism to explain species coexistence in an open and environmentally heterogeneous ecosystem. The use of MBFG classification and functional space to describe species within clumps revealed that under the same size range, species with a greater degree of redundancy alternate their dominance in an unpredictable way. The significance and dominance of the clumps were related to the environmental conditions, but the biovolume of species within the clumps was better predicted by functional distinctiveness than by pairwise functional redundancy. This addresses the difficulty to avoid the ghost of hidden niches (Barabás et al. 2013), and also provides evidence from multiple angles that points to EN as a plausible mechanism in shaping species coexistence.

Acknowledgments

CGR PhD scholarship was funded by Fudação de Apoio a Pesquisa do Estado do Rio de Janeiro (FAPERJ) and by Coordenação de Aperfeiçoamento de Pessoal de Nível Superior (CAPES). MMM was partially supported by CNPq (303572/2017-5).

References

Allen, C. R., L. Gunderson, and A. R. Johnson. 2005. The use of discontinuities and functional groups to assess relative resilience in complex systems. Ecosystems 8:958–966.

Anderson, M. J. 2006. Distance-based tests for homogeneity of multivariate dispersions. Biometrics 62:245–253.

APHA, A. 2005. WEF: Standard Methods for the Examination of Water and Wastewater: Centennial Edition. Washington, DC.

Barabás, G., R. D'Andrea, R. Rael, G. Meszéna, and A. Ostling. 2013. Emergent neutrality or hidden niches? Oikos.

Blanckenhorn, W. U. 2000. The Evolution of Body Size: What Keeps Organisms Small? The Quarterly Review of Biology 75:385–407.

Bonser, S. P. 2006. Form defining function: interpreting leaf functional variability in integrated plant phenotypes. Oikos.

Bortolini, J. C., and N. C. Bueno. 2017. Temporal dynamics of phytoplankton using the morphology-based functional approach in a subtropical river. Revista Brasileira de Botanica 40:741–748.

Chen, N., L. Liu, Y. Li, D. Qiao, Y. Li, Y. Zhang, and Y. Lv. 2015. Morphology-based classification of functional groups for potamoplankton. Journal of Limnology 74:559–571.

Clark, J. S., M. Dietze, S. Chakraborty, P. K. Agarwal, I. Ibanez, S. LaDeau, and M. Wolosin. 2007. Resolving the biodiversity paradox. Ecology Letters 10:647–659.

Cornwell, W. K., and D. D. Ackerly. 2009. Community assembly and shifts in plant trait distributions across an environmental gradient in coastal California. Ecological Monographs 79:109–126.

Coux, C., R. Rader, I. Bartomeus, and J. M. Tylianakis. 2016. Linking species functional roles to their network roles. Ecology letters 19:762–770.

D'Andrea, R., J. Guittar, J. P. O'Dwyer, H. Figueroa, S. J. Wright, R. Condit, and A. Ostling. 2020. Counting niches: Abundance-by-trait patterns reveal niche partitioning in a Neotropical forest. Ecology 101.

509 D'Andrea, R., A. Ostling, and J. P. O'Dwyer. 2018. Translucent windows: how
510 uncertainty in competitive interactions impacts detection of community pattern.
511 Ecology Letters 21:826–835.
512 Descy, J. P., F. Darchambeau, T. Lambert, M. P. Stoyneva-Gaertner, S. Bouillon, and A.
513 v. Borges. 2017. Phytoplankton dynamics in the Congo River. Freshwater Biology
514 62:87–101.
515 Díaz, S., J. Kattge, J. H. C. Cornelissen, I. J. Wright, S. Lavorel, S. Dray, B. Reu, M. Kleyer,
516 C. Wirth, I. Colin Prentice, E. Garnier, G. Bönisch, M. Westoby, H. Poorter, P. B.
517 Reich, A. T. Moles, J. Dickie, A. N. Gillison, A. E. Zanne, J. Chave, S. Joseph Wright,
518 S. N. Sheremet Ev, H. Jactel, C. Baraloto, B. Cerabolini, S. Pierce, B. Shipley, D.
519 Kirkup, F. Casanoves, J. S. Joswig, A. Günther, V. Falczuk, N. Rüger, M. D. Mahecha,
520 and L. D. Gorné. 2016. The global spectrum of plant form and function. Nature
521 529:167–171.
522 Díaz, S., A. Purvis, J. H. C. Cornelissen, G. M. Mace, M. J. Donoghue, R. M. Ewers, P.
523 Jordano, and W. D. Pearse. 2013. Functional traits, the phylogeny of function, and
524 ecosystem service vulnerability. Ecology and Evolution 3:2958–2975.
525 Dolédec, S., D. Chessel, C. J. F. ter Braak, and S. Champely. 1996. Matching species traits to
526 environmental variables: A new three-table ordination method. Environmental and
527 Ecological Statistics 3:143–166.
528 Downing, A. S., S. Hajdu, O. Hjerne, S. A. Otto, T. Blenckner, U. Larsson, and M.
529 Winder. 2014. Zooming in on size distribution patterns underlying species
530 coexistence in Baltic Sea phytoplankton. Ecology Letters 17:1219–1227.
531 Dray, S., P. Choler, S. Dolédec, P. R. Peres-Neto, W. Thuiller, S. Pavoine, and C. J. F. ter
532 Braak. 2014. Combining the fourth-corner and the RLQ methods for assessing trait
533 responses to environmental variation. Ecology 95:14–21.

534 Dray, S., and P. Legendre. 2008. Testing the species traits environment relationships: The
535 fourth-corner problem revisited. Ecology 89:3400–3412.
536 Fort, H., M. Scheffer, and E. van Nes. 2010. The clumping transition in niche
537 competition: A robust critical phenomenon. Journal of Statistical Mechanics:
538 Theory and Experiment 2010.
539 Gause, G. F. 1936. The Struggle for Existence. Soil Science 41:159.
540 Götzenberger, L., F. de Bello, K. A. Bråthen, J. Davison, A. Dubuis, A. Guisan, J. Lepš, R.
541 Lindborg, M. Moora, M. Pärtel, L. Pellissier, J. Pottier, P. Vittoz, K. Zobel, and M.
542 Zobel. 2012. Ecological assembly rules in plant communities-approaches, patterns and
543 prospects. Biological Reviews 87:111–127.
544 Graco-Roza, C., J. B. O. Santos, V. L. M. Huszar, P. Domingos, J. Soininen, and M. M.
545 Marinho. 2020. Downstream transport processes modulate the effects of
546 environmental heterogeneity on riverine phytoplankton. Science of the Total
547 Environment 703.
548 Gravel, D., C. D. Canham, M. Beaudet, and C. Messier. 2006. Reconciling niche and
549 neutrality: The continuum hypothesis. Ecology Letters.
550 Hardin, G. 1960. The Competitive Exclusion Principle.
551 Hillebrand, H., C.-D. D. Dürselen, D. Kirschtel, U. Pollingher, and T. Zohary. 1999.
552 Biovolume calculation for pelagic and benthic microalgae. Journal of Phycology
553 35:403–424.
554 Holling, C. S. 1992. Cross-Scale Morphology, Geometry, and Dynamics of Ecosystems.
555 Ecological Monographs 62:447–502.
556 Holt, R. D. 2006. Emergent neutrality. Trends in Ecology and Evolution 21:531–533.
557 Hubbell, S. P. 2001. The Unified Neutral Theory of Biodiversity and Biogeography.
558 Page Monographs in Population Biology.

559 Hubbell, S. P. 2006. Neutral theory and the evolution of ecological equivalence.
560 Hutchinson, G. E. 1957. Concluding Remarks. Cold Spring Harbor Symposia on
561 Quantitative Biology.
562 Ingram, T., R. Costa-Pereira, and M. S. Araújo. 2018. The dimensionality of individual
563 niche variation. Ecology 99:536–549.
564 Irwin, A. J., Z. v. Finkel, O. M. E. Schofield, and P. G. Falkowski. 2006. Scaling-up
565 from nutrient physiology to the size-structure of phytoplankton communities.
566 Journal of Plankton Research.
567 Junk, W. J., P. B. Bayley, and R. E. Sparks. 1989. The flood pulse concept in river-
568 floodplain systems. Canadian special publication of fisheries and aquatic sciences
569 106:110–127.
570 Kraft, N. J. B., R. Valencia, and D. D. Ackerly. 2008. Functional traits and niche-based
571 tree community assembly in an Amazonian forest. Science 322:580–582.
572 Kruk, C., V. L. M. Huszar, E. T. H. M. Peeters, S. Bonilla, L. Costa, M. LüRling, C. S.
573 Reynolds, and M. Scheffer. 2010. A morphological classification capturing
574 functional variation in phytoplankton. Freshwater Biology 55:614–627.
575 Kruk, C., E. T. H. M. Peeters, E. H. van Nes, V. L. M. Huszar, L. S. Costa, and M.
576 Scheffer. 2011. Phytoplankton community composition can be predicted best in
577 terms of morphological groups. Limnology and Oceanography 56:110–118.
578 Kruk, C., and A. M. Segura. 2012. The habitat template of phytoplankton morphology-
579 based functional groups. Hydrobiologia 698:191–202.
580 Laliberté, E., P. Legendre, B. Shipley, and M. E. Laliberté. 2014. Package 'FD.'
581 Measuring functional diversity from multiple traits, and other tools for functional
582 ecology.

583 Legendre, P., R. G. Galzin, and M. L. Harmelin-Vivien. 1997. Relating behavior to habitat:
584 Solutions to the fourth-corner problem. Ecology 78:547–562.
585 Litchman, E., K. F. Edwards, C. A. Klausmeier, and M. K. Thomas. 2012. Phytoplankton
586 niches, traits and eco-evolutionary responses to global environmental change. Marine
587 Ecology Progress Series 470:235–248.
588 Litchman, E., and C. A. Klausmeier. 2008. Trait-Based Community Ecology of
589 Phytoplankton. Annual Review of Ecology, Evolution, and Systematics 39:615–
590 639.
591 Litchman, E., P. de Tezanos Pinto, C. A. Klausmeier, M. K. Thomas, and K.
592 Yoshiyama. 2010. Linking traits to species diversity and community structure in
593 phytoplankton. Hydrobiologia 653:15–28.
594 Lund, J. W. G., C. Kipling, and E. D. le Cren. 1958. The inverted microscope method of
595 estimating algal numbers and the statistical basis of estimations by counting.
596 Hydrobiologia 11:143–170.
597 Macarthur, R., and R. Levins. 1967. The Limiting Similarity, Convergence, and
598 Divergence of Coexisting Species. The American Naturalist 101:377–385.
599 Marañón, E. 2008. Inter-specific scaling of phytoplankton production and cell size in the
600 field. Journal of Plankton Research.
601 Margalef, R. 1978. Life-forms of phytoplankton as survival alternatives in an unstable
602 environment. Oceanologica acta 134:493 509.
603 McGill, B. J., B. J. Enquist, E. Weiher, and M. Westoby. 2006. Rebuilding community
604 ecology from functional traits. Trends in Ecology and Evolution 21:178–185.
605 Mouillot, D., N. A. J. Graham, S. Villéger, N. W. H. Mason, D. R. Bellwood, Mouillot,
606 Graham, Villéger, Mason, Bellwood, D. Mouillot, N. A. J. Graham, S. Villéger, N.

607 W. H. Mason, and D. R. Bellwood. 2013. A functional approach reveals
608 community responses to disturbances. Trends in Ecology & Evolution 28:167–177.
609 Oksanen, J. 2017. Vegan: ecological diversity. R Package Version 2.4-4:11.
610 Pavoine, S., M. B. Bonsall, A. Dupaix, U. Jacob, and C. Ricotta. 2017. From
611 phylogenetic to functional originality: Guide through indices and new
612 developments. Ecological Indicators 82:196–205.
613 Reynolds, C., and J. Descy. 1996. The production biomass and structure of
614 phytoplankton in large rivers. Arch. Hydrobiol. 113:161–187.
615 Reynolds, C. S. 2006. The Ecology of Phytoplankton. Page The Ecology of
616 Phytoplankton. Cambridge University Press, Cambridge.
617 Reynolds, C. S., J. Alex Elliott, and M. A. Frassl. 2014. Predictive utility of trait-
618 separated phytoplankton groups: A robust approach to modeling population
619 dynamics. Journal of Great Lakes Research 40:143–150.
620 Reynolds, C. S., J. P. Descy, and J. Padisák. 1994. Are phytoplankton dynamics in rivers
621 so different from those in shallow lakes? Hydrobiologia 289:1–7.
622 Ricotta, C., F. de Bello, M. Moretti, M. Caccianiga, B. E. L. Cerabolini, and S. Pavoine.
623 2016. Measuring the functional redundancy of biological communities: a quantitative
624 guide. Methods in Ecology and Evolution 7:1386–1395.
625 Roy, S., and J. Chattopadhyay. 2007. Toxin-allelopathy among phytoplankton species
626 prevents competitive exclusion. Journal of Biological Systems 15:73–93.
627 Sakavara, A., G. Tsirtsis, D. L. Roelke, R. Mancy, and S. Spatharis. 2018. Lumpy
628 species coexistence arises robustly in fluctuating resource environments.
629 Proceedings of the National Academy of Sciences of the United States of America
630 115:738–743.

631 Sauterey, B., B. Ward, J. Rault, C. Bowler, and D. Claessen. 2017. The implications of
632 eco-evolutionary processes for the emergence of marine plankton community
633 biogeography. The American Naturalist 190:116–130.
634 Scheffer, M., and E. H. van Nes. 2006. Self-organized similarity, the evolutionary
635 emergence of groups of similar species. Proceedings of the National Academy of
636 Sciences.
637 Scheffer, M., E. H. van Nes, and R. Vergnon. 2018. Toward a unifying theory of
638 biodiversity. Proceedings of the National Academy of Sciences of the United States
639 of America 115:639–641.
640 Scheffer, M., R. Vergnon, E. H. van Nes, J. G. M. Cuppen, E. T. H. M. Peeters, R. Leijs,
641 and A. N. Nilsson. 2015. The Evolution of Functionally Redundant Species;
642 Evidence from Beetles. PLOS ONE 10:e0137974.
643 Segura, A. M., D. Calliari, C. Kruk, D. Conde, S. Bonilla, and H. Fort. 2011. Emergent
644 neutrality drives phytoplankton species coexistence. Proceedings of the Royal
645 Society B: Biological Sciences 278:2355–2361.
646 Segura, A. M., C. Kruk, D. Calliari, F. García-Rodriguez, D. Conde, C. E. Widdicombe,
647 and H. Fort. 2013. Competition drives clumpy species coexistence in estuarine
648 phytoplankton. Scientific Reports 3:1–6.
649 Soares, M. C. S., V. L. M. Huszar, and F. Roland. 2007. Phytoplankton dynamics in two
650 tropical rivers with different degrees of human impact (southeast Brazil). River
651 Research and Applications 23:698–714.
652 Sun, J., and D. Liu. 2003. Geometric models for calculating cell biovolume and surface area
653 for phytoplankton. Journal of Plankton Research 25:1331–1346.

Thibault, K. M., E. P. White, A. H. Hurlbert, and S. K. M. Ernest. 2011. Multimodality in the individual size distributions of bird communities. Global Ecology and Biogeography.

Uhelingher, V. 1964. Étude statistique dês méthodes de dénobrement planctonique. Archives des Sciences 77:121–123.

Utermöhl, H. 1958. Zur Vervollkommnung der quantitativen Phytoplankton-Methodik. SIL Communications, 1953-1996 9:1–38.

Vannote, R. L., G. W. Minshall, K. W. Cummins, J. R. Sedell, and C. E. Cushing. 1980. The River Continuum Concept. Canadian Journal of Fisheries and Aquatic Sciences 37:130–137.

Vergnon, R., N. K. Dulvy, and R. P. Freckleton. 2009. Niches versus neutrality: Uncovering the drivers of diversity in a species-rich community. Ecology Letters 12:1079–1090.

Violle, C., M.-L. Navas, D. Vile, E. Kazakou, C. Fortunel, I. Hummel, and E. Garnier. 2007. Let the concept of trait be functional! Oikos 116:882–892.

Violle, C., W. Thuiller, N. Mouquet, F. Munoz, N. J. B. Kraft, M. W. Cadotte, S. W. Livingstone, and D. Mouillot. 2017. Functional Rarity: The Ecology of Outliers. Trends in Ecology and Evolution 32:356–367.

Wang, C., X. Li, Z. Lai, Y. Li, A. Dauta, and S. Lek. 2014. Patterning and predicting phytoplankton assemblages in a large subtropical river. Fundamental and Applied Limnology / Archiv für Hydrobiologie 185:263–279.

Wetzel, R. G. 2001. Limnology: Lake and River Ecosystems. Third edition. Academic Press.